

High speed optical modulation of terahertz waves using annealed silicon wafer

Tao Li (李 涛)¹, Dongxiao Yang (杨冬晓)^{1,2*}, and Jian Wang (王 健)¹

¹Department of Information Science and Electronic Engineering, Zhejiang University, Hangzhou 310027, China,

²Research Center for Terahertz Technology, Zhejiang University, Hangzhou 310027, China

*Corresponding author: yangdx@zju.edu.cn

Received March 5, 2014; accepted May 20, 2014; posted online July 18, 2014

Modulation properties of terahertz waves going through a light excited high resistivity silicon wafer are analyzed and measured. Free carrier lifetime of the silicon wafer affects the modulation depth and speed of the terahertz wave. The lifetime is reduced to less than 1 μs by thermal processing for high speed modulation. Experimental results show that the response time and modulation depth of the proposed modulating structure are close to 1 μs and 51%, respectively.

OCIS codes: 250.4110, 300.6495, 160.6000.

doi: 10.3788/COL201412.082501.

In recent years, with the rapid development of terahertz (THz) wave generators and detectors, THz electromagnetic radiation with the frequency ranging from 0.1 to 10 THz has attracted a great deal of attention for its unique applications in the fields of imaging, detection, and communication^[1–4]. But technical challenges still exist and some typical functional devices for THz applications such as filters^[5], waveguides^[6], splitters^[7], and modulators are required for further research. Rahm *et al.*^[8] reviewed different techniques for modulation of THz waves and optical modulation using high resistivity semiconductors, such as Si and GaAs, showed a big potential. In 2007, Fekete *et al.*^[9] demonstrated a THz modulator based on a one-dimensional photonic crystal with a GaAs wafer inserted in the middle as a defect layer, which enabled an efficient optical modulation of THz beam. In the same year, Chen *et al.*^[10] demonstrated optical switching of electrically resonant THz planar metamaterials fabricated on ErAs/GaAs nanoisland superlattice substrates with a switching recovery time of 20 ps. However, the structure of the two THz devices is a little complicated. In 2009, Li^[11] proposed a novel optical controllable THz wave modulator using a single silicon wafer, but the response time was about 5 ms, which was very long for THz communication. In 2013, Cheng *et al.*^[12] reported optical modulation of continuous THz wave using photo-induced reconfigurable patterns on a silicon wafer, and the modulation speed was 1.3 kHz limited by the illumination system.

In this letter, we shorten the carrier lifetime of the high resistivity silicon wafer, which is relatively long, to less than 1 μs by thermal processing. This improvement enables high speed modulation up to 500 kHz. The response time of the proposed modulating structure is close to 1 μs and the gain is a factor of 5000 compared with the result reported by Li^[11].

When a high resistivity silicon wafer is excited by optical beam with photon energy higher than its band-gap energy, free carriers can be generated and induce a dramatic increase of the imaginary part of the permittivity. The silicon wafer becomes not transparent for THz wave, and hence it is possible to control the transmit-

tance of THz wave through the silicon wafer by changing the power of the exciting optical beam. The lifetime of the photo-excited free carriers is an important parameter of the modulation mechanism. The modulation response time depends on the generation and recombination time of the photo-excited free carriers. Usually photo-excited free carriers can be generated in a very short time such as several nanoseconds but disappear in a much longer time because silicon is an indirect-transition semiconductor. The free carrier lifetime in high resistivity silicon wafer is determined by impurity recombination and the time constant is relatively long, in tens of microseconds^[13]. So the free carrier lifetime determines the maximum modulation speed and it must be short enough for high speed modulation applications.

At high temperature, transition metals such as copper, iron, and nickel have high diffusion coefficients. They can diffuse into the silicon bulk easily, introducing deep levels in the silicon band gap and reducing the free carrier lifetime dramatically^[14]. The wafer used is 3 inches *n*-type <100> silicon with the thickness of about 300 μm . The resistivity is larger than 8000 $\Omega\cdot\text{cm}$ and the free carrier lifetime is about 5.2 μs . The experimental sample with a size of 1×1.5 (cm) was cut from the wafer. After dropping $\text{Cu}(\text{NO}_3)_2$ solution on the surface, the sample was placed into a conventional furnace to drive in the Cu impurities in an Ar ambient at 900°C for 2 h, followed by cooling with a rate of 10 K/min. Then, the sample surfaces were chemically polished to remove the remained Cu contaminants. Through the above processing the free carrier lifetime of the silicon wafer was shortened to less than 1 μs . Figure 1(a) shows the free carrier lifetime distribution of the annealed silicon wafer measured by microwave photoconductivity decay method. Figure 1(b) is the histogram of the occupied surface area percentages of different free carrier lifetimes. It is seen that the free carrier lifetime is not distributed evenly throughout the whole silicon wafer, which is caused by the ununiformity of the dropped $\text{Cu}(\text{NO}_3)_2$ solution in this experiment. The central area has a low lifetime of 0.7 μs and it can provide a short modulating response time.

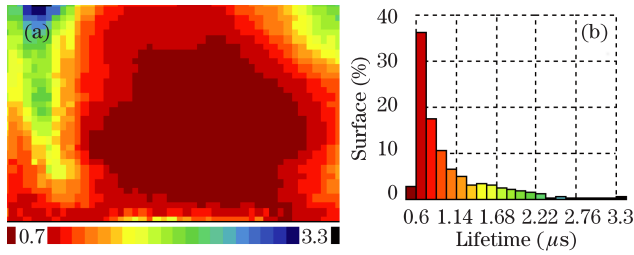


Fig. 1. (Color online) Free carrier lifetime of the annealed silicon wafer measured by microwave photoconductivity decay method. (a) Distribution diagram and (b) histogram of the occupied surface area percentages of different free carrier lifetimes.

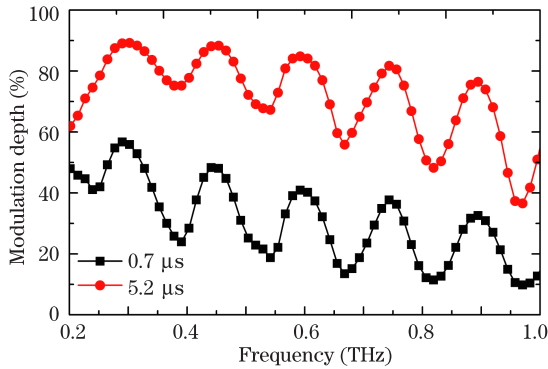


Fig. 2. (Color online) Modulation depths of the silicon wafer before and after the thermal processing.

Modulation depths of the silicon wafer before and after the thermal processing are measured using a THz time domain spectrometer. The silicon wafer, placed at the focus of the THz wave beam, is excited by an infrared laser (808 nm) with a constant output intensity of 2 W/cm^2 . The modulation depth is determined from $M = (T_{\max} - T_{\min}) / (T_{\max} + T_{\min}) \times 100\%$, where T_{\max} and T_{\min} are the THz powers when the exciting light source is off and on, respectively. Figure 2 shows the experimental results. The black line marked with square and the red line marked with solid circle are modulation depths of the silicon wafer before and after the thermal processing, respectively. The photo-excited carrier density in high-resistivity silicon wafer is related to the carrier lifetime, which can be calculated using the equation $n_{\text{ph}} = \tau P_{\text{ex}} \alpha (1 - R) / (h\nu q)$, where τ and P_{ex} are carrier lifetime and exciting light intensity, respectively^[12]. The expression indicates that at the same exciting laser intensity, the longer the carrier lifetime is, the higher the photo-excited carrier density it induces. According to the Drude model, photo-excited carrier density contributes to increase of the imaginary part of the permittivity, which means that the higher the photo-excited carrier density is, the larger attenuation of THz waves going through the silicon wafer it causes. Therefore, the achieved modulation depth will be high when the carrier lifetime is long. The periodic fluctuation of the modulation depth in Fig. 2 is caused by the Fabry-Perot effect between the two surfaces of the silicon wafer. The frequency interval Δf should satisfy: $\Delta f = c/2nd$, where c is the light speed, n is the refractive

index of the silicon, and d is the thickness of the silicon wafer. Here, the measured refractive index ranges from 3.23 to 3.47 at 0.3–1.0 THz. A middle value 3.35 is used for approximate analysis of the Fabry-Perot effect, and $d = 300 \mu\text{m}$, so $\Delta f = 0.149 \text{ THz}$, which matches the experimental results. Apparently, for silicon wafer with short free carrier lifetime, large modulation depth can be achieved by enhancing the power of the exciting laser beam.

Figure 3 shows the schematic of the proposed THz wave modulation experiment system. A backward-wave oscillator (BWO) is used as THz wave source. The output frequency is set to be 0.35 THz, which is the low air loss window of the THz waves. Annealed silicon wafer is placed at the focus of the THz beam as the key device of the modulation structure. A continuous wave infrared laser (808 nm) is used as the source of the exciting light, which is modulated by a free-space electro-optic amplitude modulator (EO-AM-NR-C1, Thorlabs, USA) and a high voltage power supply is used to drive the electro-optic modulator. The modulated laser beam is split into two beams by a piece of glass. A low power beam is detected by a photodetector to monitor the modulation depth of the exciting light. The other laser beam is used to excite the front surface of the silicon wafer. To make sure that the entire THz wave passing through the silicon wafer is attenuated by the photo-excited free carriers, a thin metal aperture with diameter of 2 mm as the same as the diameter of exciting laser beam is placed in front of the silicon wafer. The modulated THz wave is detected using a high sensitive zero-bias schottky diode detector (Virginia Diodes Inc., USA). The driving voltage, modulated laser beam power and modulated THz wave power are measured in real-time using an oscilloscope.

Figure 4 shows the experimental results. The blue line is the driving voltage of the free-space electro-optic amplitude modulator and the half-wave driving voltage is about 280 V. The red line is part of the modulated exciting laser beam power, used to monitor the modulation depth of the laser beam, which is about 60% in the experiment. The average optical power exciting the front surface of the silicon wafer is 4 W/cm^2 measured by an optical power meter. The black line is the power waveform of the modulated THz wave. The modulation frequency is 0.1 MHz as showed with the rise and fall times of 1.15 and $0.95 \mu\text{s}$, respectively. The response time of the modulation structure is limited by the lifetime of the light excited free carriers and the response time of the high voltage driving power supply. Due to the

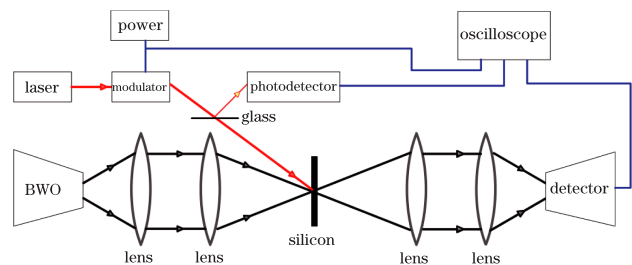


Fig. 3. (Color online) Schematic of the proposed THz wave modulation experiment system. The black line, red line, and blue line represent THz wave path, infrared light path, and electrical signal line, respectively.

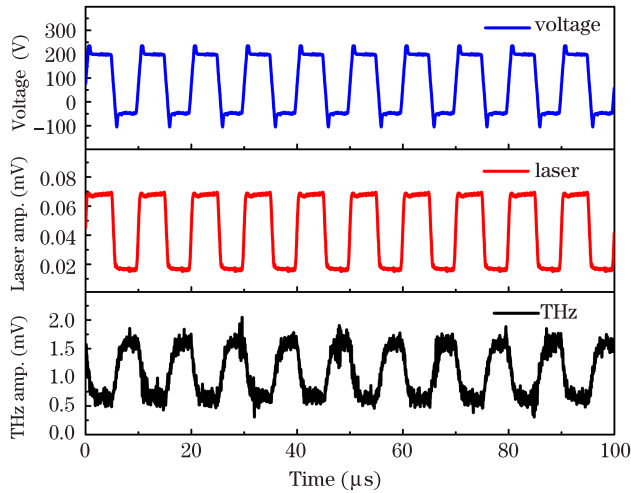


Fig. 4. (Color online) Measured driving voltage, modulated laser power, and modulated THz wave power at the modulation frequency of 0.1 MHz.

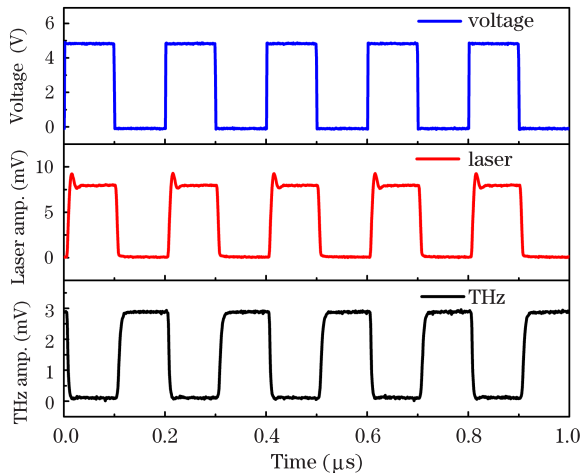


Fig. 5. (Color online) Measured TTL signal, internal modulated laser power, and modulated THz wave power at the modulation frequency of 5 kHz.

performance of the power supply at higher frequency, the measured modulation speed is hard to enhance. However, according to the rise and fall time, the maximum modulation speed can be expected to about 0.5 MHz. It can be seen from Fig. 4 that for modulated THz wave: $T_{\max} = 1.68$ mV, $T_{\min} = 0.54$ mV. Therefore, the modulation depth of the proposed THz modulation structure is about 51%. The modulation depth of THz waves is related to the intensity and the modulation depth of the exciting laser beam. Because of the limitation of the laser beam and the electro-optic modulator, the modulation depth of the modulated exciting laser beam is only 60%, which restricts the achievement of the maximum modulation depth.

At a low modulation frequency, an exciting light with modulation depth of 100% is realized by using a Transistor-Transistor Logic (TTL) signal to drive the internal modulation of the laser. In this case, the electro-optic modulator in Fig. 3 is not needed. Figure 5 shows

the experimental results at the modulation frequency of 5 kHz. The blue line is the measured TTL voltage. The high voltage and low voltage are 5 and 0 V, respectively. The red line is part of the internal modulated laser power. The high and low light powers exciting the silicon wafer are 20 and 0 W/cm², respectively. The black line is the power waveform of the modulated THz wave with $T_{\max} = 2.90$ mV and $T_{\min} = 0.10$ mV. The achieved modulation depth is about 93%, which means that large modulation depth of THz waves at high frequency can also be achieved with proper exciting laser beam.

In conclusion, based on light induced absorption of THz waves in high resistivity silicon wafer, the modulation properties of the structure are experimentally demonstrated. By thermal processing the free carrier lifetime of the silicon wafer is reduced for high speed modulation. Experiment results show that the response time of the proposed modulation structure is close to 1 μ s and the THz wave modulation depth reaches 51% in a broad frequency band ranging from 0.2 to 1 THz. It is believed that the modulation properties of the demonstrated structure can be useful for future THz wave sensor and communication systems.

This work was supported by the National Natural Science Foundation of China under Grant Nos. 60671006 and 60971059. The authors would like to thank Associate Researcher X. G. Yu of State Key Laboratory of Silicon Materials of Zhejiang University for the thermal processing of silicon wafer.

References

1. P. H. Siegel, *IEEE Trans. Microw. Theor. Technol.* **50**, 910 (2002).
2. I. Hosako, N. Sekine, M. Patrashin, S. Saito, K. Fukunaga, Y. Kasai, P. Baron, T. Seta, J. Mendrok, S. Ochiai, and H. Yasuda, *Proc. IEEE* **95**, 1611 (2007).
3. J. Federici and L. Moeller, *J. Appl. Phys.* **107**, 111101 (2010).
4. Z. Tan, Z. Chen, J. Cao, and H. Liu, *Chin. Opt. Lett.* **11**, 031403 (2013).
5. L. Rao, D. X. Yang, L. Zhang, T. Li, and S. Xia, *Appl. Opt.* **51**, 912 (2012).
6. L. Rao, D. X. Yang, and Z. Hong, *Microw. Opt. Technol. Lett.* **54**, 2856 (2012).
7. M. Zhang, X. Li, S. Liang, P. Liu, J. Liu, and Z. Hong, *Chin. Opt. Lett.* **11**, 122301 (2013).
8. M. Rahm, J. Li, and W. J. Padilla, *J. Infrared Milli Terahz Waves* **34**, 1 (2013).
9. L. Fekete, F. Kadlec, P. Kužel, and H. Nemeč, *Opt. Lett.* **32**, 680 (2007).
10. H. T. Chen, W. J. Padilla, J. M. Zide, S. R. Bank, A. C. Gossard, A. J. Taylor, and R. D. Averitt, *Opt. Lett.* **32**, 1620 (2007).
11. J. Li, *Microw. Opt. Technol. Lett.* **51**, 2825 (2009).
12. L. Cheng and L. Liu, *Opt. Express* **21**, 28657 (2013).
13. T. Nozokido, H. Minamide, and K. Mizuno, *Electron. Commun. Jp. Part 2 Electron* **80**, 1 (1997).
14. A. A. Istratov, H. Hieslmair, and E. R. Weber, *Appl. Phys. A* **70**, 489 (2000).